Biochemical and Biophysical Research Communications **281,** 172–179 (2001)
doi:10.1006/bbrc.2001.4331, available online at http://www.idealibrary.com on IDEAL®

Spontaneous and Flow-Induced Ca^{2+} Transients in Retracted Regions in Endothelial Cells

Takurou Miyazaki, Hisayuki Ohata, Masayuki Yamamoto, and Kazutaka Momose
Department of Pharmacology, School of Pharmaceutical Sciences, Showa University, Hatanodai, Shinagawa-ku, Tokyo 142-8555, Japan

Received January 9, 2001

Changes in intracellular calcium concentration ($[Ca^{2+}]_i$) and focal adhesion sites of cultured bovine aortic endothelial cells (BAECs) were simultaneously visualized in real time. Local $[Ca^{2+}]_i$ transients were observed at the rear edges of spontaneously migrating BAECs. Furthermore, the majority of starting regions of $[Ca^{2+}]_i$ transients retracted continuously. Frequency of $[Ca^{2+}]_i$ transients increased with the application of fluid flow. The majority of starting regions of flow-induced $[Ca^{2+}]_i$ transients retracted following the occurrence of $[Ca^{2+}]_i$ transients. In addition, retracted areas were distributed in the upstream regions of the cell. Application of $GdCl_3$, a mechanosensitive cation channel blocker, resulted in a clear reduction of $[Ca^{2+}]_i$ transients and rear retractions in cases of spontaneous and flow-induced BAEC migration. Flow-induced directional rear retractions were also inhibited. Consequently, we conclude that local $[Ca^{2+}]_i$ transients play an important role in the migration of BAECs with respect to rear retraction. Furthermore, flow-induced $[Ca^{2+}]_i$ transients regulate directional rear retraction under flow conditions. © 2001 Academic Press

Key Words: **mechanotransduction; Ca^{2+} transient; endothelial cell; retraction; migration; fluid flow; spontaneous; gadolinium; focal adhesion; integrin.**

Migration of vascular endothelial cells (ECs) is believed to be of paramount importance in biological processes, including angiogenesis (1) and wound healing (2). Spontaneous morphological changes in cultured ECs exhibit a random-walk pattern. However, EC motility patterns are altered under fluid shear stress. Changes are characterized by the development of leading edges (lamellipodia) in the direction of flow (3). Elongation and alignment in the direction of flow have also been observed in ECs (4). Changes in $[Ca^{2+}]_i$ have an important role with respect to these motility processes, such as the production of actin-myosin-based contraction forces (5), the regulation of the structure and dynamics of the actin cytoskeleton (6) as well as formation (7) and disassembly (8) of cell-substratum adhesion.

The relationship between changes in $[Ca^{2+}]_i$ and cell motility has been investigated in several cell types, including keratocytes and neutrophils. $[Ca^{2+}]_i$ transients have been described in chemotactic neutrophils. Additionally, $[Ca^{2+}]_i$ transients and cell migration were inhibited by buffering of intracellular Ca^{2+} (9). $[Ca^{2+}]_i$ transients were also demonstrated in spontaneously migrating keratocytes. Stretch-activated Ca^{2+} channel involvement was noted (10). It is clear that changes in $[Ca^{2+}]_i$ were involved in motility processes in these cell types; however, the exact mechanisms regarding the regulation of EC morphology by spontaneous and flow-induced $[Ca^{2+}]_i$ transients remain unclear. Furthermore, $[Ca^{2+}]_i$ transients in spontaneously migrating ECs have not been reported.

In this study, $[Ca^{2+}]_i$ and focal adhesion sites evident in spontaneously and flow-induced migrating BAECs were visualized with confocal and interference reflection microscopy. The details of the relationship between the spatiotemporal properties of changes in $[Ca^{2+}]_i$, cell morphology and cell-substratum adhesion were investigated. Our visualized data demonstrated, for the first time, the occurrence of local $[Ca^{2+}]_i$ transients at cell-substratum adhesion sites at the rear edges of BAECs followed by retraction.

MATERIALS AND METHODS

Materials. Fluo-4-acetoxymethylester (fluo-4/AM), fura-red-acetoxymethylester (fura-red/AM), and calcein-acetoxymethylester (calcein/AM) were purchased from Molecular Probes, Inc. (Eugene, OR). Fetal bovine serum (FBS) was acquired from Intergen Company (Purchase, NY). Minimum essential medium (MEM) and trypsin-EDTA were obtained from Gibco, Inc. (Grand Island, NY). Fibronectin was purchased from Nitta Geratin, Inc. (Yao, Osaka, Japan). $GdCl_3$ was obtained from Wako Pure Chemicals (Osaka, Japan). All other chemicals were commercial products of the highest available

0006-291X/01 $35.00

grade of purity. Bovine aortic endothelial cells (BAECs) were provided by Dr. S. Shimizu (Dept. of Pathophysiology, School of Pharmaceutical Sciences, Showa University).

Cell culture. Established BAECs (11) were cultured in MEM containing 10% FBS under humidified conditions (95% air, 5% CO_2) at 37°C. Following trypsinization, cells were plated onto coverslips coated with 0.5 mg/ml fibronectin and cultured until subconfluence was achieved. The subconfluent cells from 12 to 28 passages were utilized in the experiments.

Loading of fluorescent probe. Microscopic chambers were constructed by punching a hole in the bottoms of 35 mm tissue culture dishes. A coverslip was attached to the bottom of the dish with silicon rubber sealant. $[Ca^{2+}]_i$ was determined in the following manner. Cultured cells on a coverslip were rinsed three times with Tyrode-Hepes buffer (THB: 137 mM NaCl, 2.7 mM KCl, 1.8 mM $CaCl_2$, 1.0 mM $MgCl_2$, 5.6 mM Hepes, 8.4 mM glucose; pH 7.4). Following rinsing, the cells were then incubated for 40 min at room temperature in the same buffer containing 5 μM fluo-4/AM.

To confirm the effects of cell thickness and localization of fluorescent probe on flow-induced $[Ca^{2+}]_i$ transients, BAECs were loaded with 5 μM fura-red/AM for 60 min, and with 0.1 μM calcein/AM for 10 min at room temperature, simultaneously (Fig. 4).

Measurement of $[Ca^{2+}]_i$. Following loading of fluo-4/AM, cells were rinsed three times with THB. Subsequently, chambers were placed on the microscopy stage. Fluorescence images were collected at room temperature employing laser scanning confocal microscopy (LSCM: MRC-500, Bio-Rad). An excitation wavelength of 488 nm was provided by an Argon-Krypton laser. Attenuation was effected with a 3–10% neutral density filter in order to minimize photodamage. Fluo-4 fluorescence images were obtained using a 510-nm long pass emission filter and a 60 x-oil immersion objective lens (1.4NA) at 0.3–0.7-sec intervals for 1–2 min. Fure-red and calcein fluorescence images were simultaneously obtained using a 660-nm long pass emission filter and a 503–553-nm band pass emission filter, respectively.

Observation of cell motility. Changes in BAEC motility and substratum were observed in the following manner. The LSCM operated on principles similar to interference reflection microscopy (IRM). That is, light is reflected from the aqueous layer lying between the cell membrane and substratum when the two materials are apart. When the two materials are in close apposition, reflected radiance levels decline sharply and the focal contacts appear dark gray-to-black in IRM images (12). Reflection was obtained utilizing a reflection mirror and a 60 x-oil immersion objective lens (1.4NA). IRM images were collected before and after $[Ca^{2+}]_i$ measurements at 3-min intervals for 14–34 min. No detectable differences were observed in the migration of fluo-4-loaded cells.

Application of fluid flow and Gd^{3+}. THB flow onto cells was effected from a pipette tip (13). The tip (inner diameter: 500 μm) was placed parallel to the coverslip at a distance of 300 μm from the centerpoint of the observed field. Pipette solution was driven by a peristaltic pump (Atto, Tokyo, Japan). Flow speed was controlled at 23.8–32.6 cm/s. Homogeneous distribution of a nonturbulent stream over the observed cells was confirmed by measuring calcein-loaded blood cells flown from a pipette tip.

Under these conditions, cells were considered to be exposed to mechanical stress displaying a shear stress component. Maximum values for shear stress (τ) were estimated (14) from the following equation:

$$\tau = 4\mu Q \pi^{-1} r^{-3},$$

where r represents radius of the pipette tip, Q the flow rate (0.047–0.063 cm^3/sec) and μ the viscosity of THB (0.009 P). Calculated values for τ ranged from 34.2 to 46.5 dyn/cm^2. Values obtained for τ occur within the physiological range or are slightly higher.

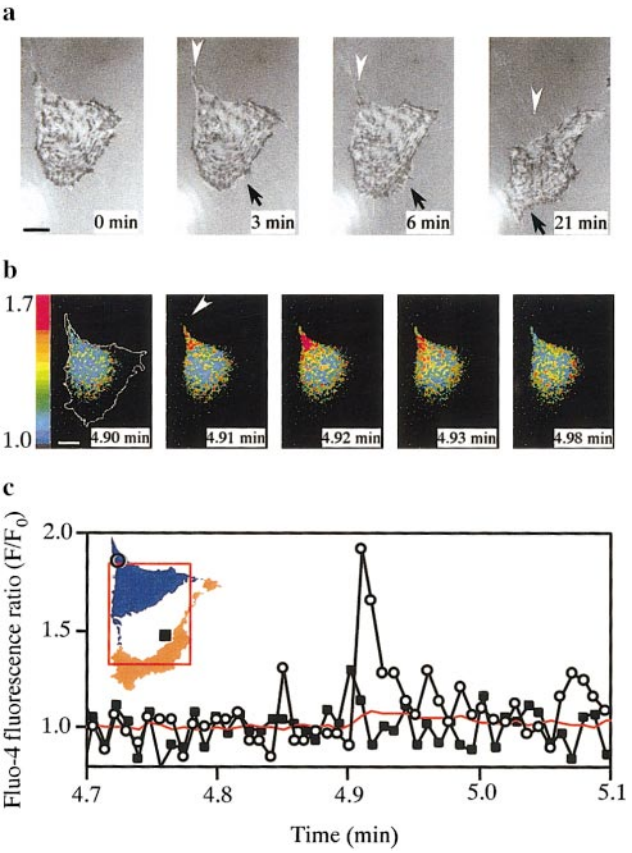

FIG. 1. Typical changes in $[Ca^{2+}]_i$ and morphology in spontaneously migrating BAECs. (a) IRM images were acquired from 0 to 21 min. The white arrowheads indicate the disappearance of cell-substratum adhesion. The black arrows indicate extended lamellipodium. Scale bar represents 10 μm. (b) Fluo-4 fluorescence ratio images. Fluorescence images were acquired from 4.7 to 5.1 min at 0.51-s intervals. Color scale is shown as F/F_0. The arrowhead indicates the starting region of $[Ca^{2+}]_i$ transient. Scale bar represents 10 μm. (c) Time course of spontaneous changes in $[Ca^{2+}]_i$. Measured regions of $[Ca^{2+}]_i$ are demonstrated in the image displaying changes in cell edges from 0 to 21 min (retraction, blue area; extension, orange area). The open circle indicates changes in $[Ca^{2+}]_i$ at the starting region of $[Ca^{2+}]_i$ transient. The closed square indicates changes in $[Ca^{2+}]_i$ in other regions of the cell. The red line represents changes in $[Ca^{2+}]_i$ of the entire cell.

In order to test the effect of Gd^{3+}, THB in the chamber and the pipette solution were replaced with the same buffer containing 30 μM $GdCl_3$.

Analysis of data. Changes in $[Ca^{2+}]_i$ were expressed as the ratio of fluorescence intensities to baseline (F/F_0). Statistical analyses were restricted to cells which exhibited clear increases in $[Ca^{2+}]_i$ (peak ratio value: 1.5–10.0, duration: 1–10 s). Rate of cell response, frequency, peak value and duration of $[Ca^{2+}]_i$ transients were calculated, respectively. Cell edges were traced in order to analyze cell motility and the rate of disappearance of areas of cells was calculated. Utilizing these values, retractions were expressed as relative retraction (Figs. 2 and 4) and distribution of retracted areas (Fig. 5). These values were determined using NIH Image software (NIH, Bethesda, MD) and expressed as mean ± SEM.

TABLE 1

Morphological Changes at the Starting Regions of $[Ca^{2+}]_i$ Transients

Motility patterns	Number of starting regions (% of total)	
	Spontaneous	Flow condition
Retraction	13 (81.3)	37 (52.1)
Termination of extension	—	11 (15.5)
Extension	1 (6.3)	2 (2.8)
No morphological changes	2 (12.5)	13 (18.3)
Indistinguishable	—	8 (11.3)

RESULTS AND DISCUSSION

Spontaneous $[Ca^{2+}]_i$ Transients in Retracted Areas in Migrating BAECs

Changes in $[Ca^{2+}]_i$ and morphology were evident in spontaneously migrating BAECs (Fig. 1). In this case, spontaneous extension of lamellipodia (black arrows in Fig. 1a) and retraction of rear edges (white arrowheads in Fig. 1a) occurred continuously. Cell-substratum adhesion was apparent in the extended regions. Adhesion disappeared in the retracted regions. $[Ca^{2+}]_i$ transients were detected simultaneously in the same cells (Figs. 1b and 1c). During spontaneous migration, $[Ca^{2+}]_i$ transients were observed locally, in areas which corresponded to retracted regions as illustrated by the white arrowheads in Fig. 1a.

Eighty-three cells were analyzed. $[Ca^{2+}]_i$ transients were detected in 16 cells (19.8%). Most of these $[Ca^{2+}]_i$ transients demonstrated a Ca^{2+}-wave-like shape. Furthermore, the transients initiated from the cell edges. $[Ca^{2+}]_i$ transient frequency was 0.211 ± 0.058/cell/min

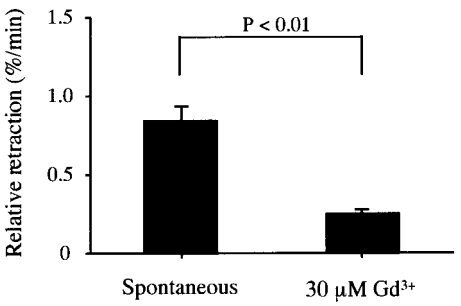

FIG. 2. Effects of Gd^{3+} on rear edge retractions in spontaneously migrating BAECs. Relative retraction was defined as the percentage of the retracted areas for 14–34 min to the entire cell area at the initiation of each image. Values were normalized by time (min) and were calculated from randomly extracted cells. Results were expressed as the mean ± SEM (control, n = 26 cells derived from 11 independent experiments; Gd^{3+}, n = 22 cells derived from 5 independent experiments). Statistical analysis was performed utilizing Student's t test.

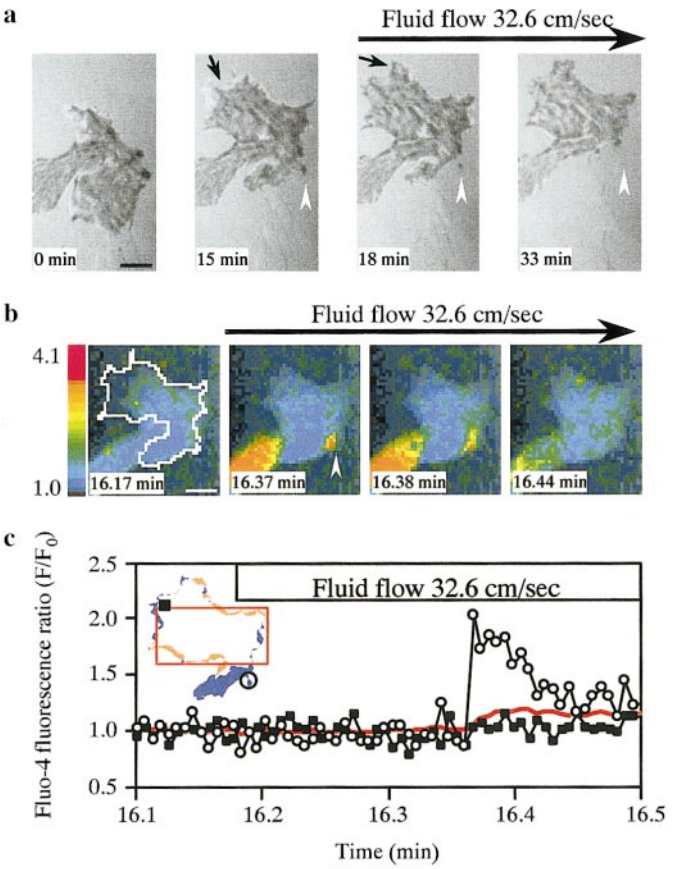

FIG. 3. Typical changes in cell morphology and $[Ca^{2+}]_i$ under flow conditions. Fluid flow was applied from 16.18 min at 32.6 cm/s. Flow direction was left to right. (a) IRM images were acquired from 0 to 33 min. The white arrowheads indicate the disappearance of cell-substratum adhesion. The black arrows indicate extended lamellipodia. Scale bar represents 10 μm. (b) Images of Fluo-4 fluorescence ratio. Fluorescence images were acquired from 16.1 to 16.5 min at 0.38-s intervals. Color scale is shown as F/F_0. The arrowhead indicates the starting region of $[Ca^{2+}]_i$ transient. Scale bar represents 10 μm. (c) Time course of flow-induced changes in $[Ca^{2+}]_i$. Measured regions of $[Ca^{2+}]_i$ are demonstrated in the image displaying changes in cell edges from 18 to 33 min (retractions, blue areas; extensions, orange areas). The open circle indicates changes in $[Ca^{2+}]_i$ at the starting region of $[Ca^{2+}]_i$ transient. The closed square indicates changes in $[Ca^{2+}]_i$ in other regions of the cell. The red line represents changes in $[Ca^{2+}]_i$ of the entire cell.

(n = 19 independent experiments) during the $[Ca^{2+}]_i$ measurement period of 1–2 min. The peak value of F/F_0 was 1.83 ± 0.14 and the duration was 3.03 ± 0.53 s in the 16 responding cells (n = 21 responses). The peak $[Ca^{2+}]_i$ levels in the majority of starting regions were higher than those observed for other regions. Morphological changes exhibited by the starting regions of $[Ca^{2+}]_i$ transients were analyzed in order to investigate the relationship between changes in $[Ca^{2+}]_i$ and cell morphology. The majority of starting regions retracted following the occurrence of $[Ca^{2+}]_i$ transients as shown in Fig. 1 (81.3%, Table 1). This high correlation between starting regions of $[Ca^{2+}]_i$ transients and re-

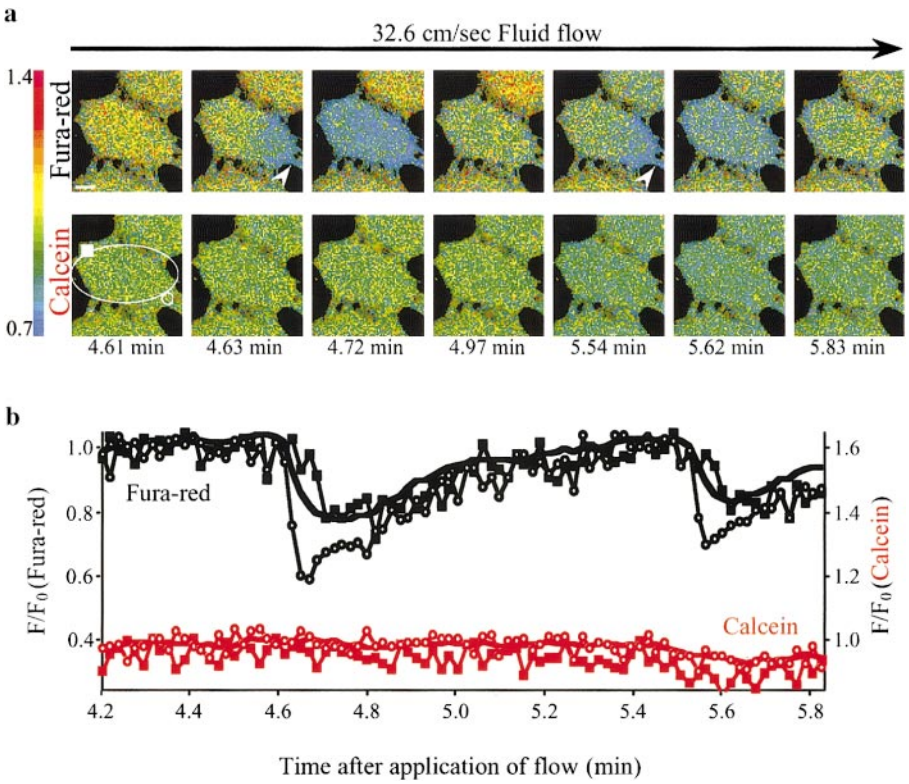

FIG. 4. Differences between changes in fura-red and calcein fluorescence in BAECs under flow conditions. Cells were loaded with 5 μM fura-red and 0.1 μM calcein simultaneously. Fluid flow was applied from 0 min at 32.6 cm/s. Flow direction was left to right. (a) Fura-red and Calcein fluorescence ratio images were acquired simultaneously at 2.24-s interval. Color scale represents F/F_0. Scale bar represents 10 μm. The white arrowheads indicate the starting region of $[Ca^{2+}]_i$ transient. (b) Time course of flow-induced changes in fluorescence. Measured regions of fluorescence are indicated in the Calcein fluorescence image as shown in a. The open circle indicates changes in F/F_0 at the starting region of $[Ca^{2+}]_i$ transient. The closed square indicates changes in F/F_0 in other regions of the cell. The lines represent changes in F/F_0 of the entire cell. The black symbols indicate changes in F/F_0 of fura-red. The red symbols indicate changes in F/F_0 of calcein.

tracted regions is the first direct evidence indicating that these processes are closely related in BAECs. Low frequency and short duration of $[Ca^{2+}]_i$ transients are believed to explain the lack of previous observation of this correlation.

A solution containing Gd^{3+} (30 μM), a mechanosensitive cation channel blocker (15), was applied to spontaneously migrating BAECs (Fig. 2), in order to determine the mechanism by which $[Ca^{2+}]_i$ transients arose. Gd^{3+}-treated cells exhibited no $[Ca^{2+}]_i$ transient during the $[Ca^{2+}]_i$ measurement period of 1–2 min (41 cells derived from 5 independent experiments). These Gd^{3+}-treated cells demonstrated significant reduction of the relative retracted area (0.25 ± 0.03%/min, $n = 22$ cells derived from 5 independent experiments; $P < 0.01$) in comparison to that observed in untreated cells (0.79 ± 0.10%/min, $n = 26$ cells derived from 11 independent experiments). These results suggest that mechanosensitive cation channels are involved in spontaneous $[Ca^{2+}]_i$ transients. Furthermore, these $[Ca^{2+}]_i$ transients are required for rear retraction in spontaneously migrating BAECs.

In studies involving keratocytes (10), spontaneous $[Ca^{2+}]_i$ transients were induced by mechanical forces generated by cytoskeletal tension. Upon keratocyte elongation, cytoskeletal tension was concentrated at the rear edges of the cell. Consequently, concentrated mechanical forces induced activation of Gd^{3+}-sensitive mechanosensitive cation channels. Spontaneous $[Ca^{2+}]_i$ transients of BAECs were visualized in local regions at rear edges. Additionally, these transients are associated with mechanosensitive cation channels. As a result, these findings suggest that spontaneous $[Ca^{2+}]_i$ transients of BAECs may also be induced by cytoskeletal tension.

Flow-Induced $[Ca^{2+}]_i$ Transients and Cell Morphology

Changes in $[Ca^{2+}]_i$ and morphology were also examined in BAECs under flow conditions in order to elucidate cell morphology regulation in the presence of mechanical stress (Fig. 3). Under these conditions, extension of the leading edges against flow direction was halted (black arrows in Fig. 3a). Furthermore, retraction of the rear edge was observed (white arrow-

heads in Fig. 3a). A local $[Ca^{2+}]_i$ transient was also evoked by application of flow during $[Ca^{2+}]_i$ measurement for 0.4 min (Figs. 3b and 3c). Additionally, the starting region of the $[Ca^{2+}]_i$ transients (arrowhead in Fig. 3b) corresponded to focal adhesion sites (black plaques indicated by a white arrowhead in Fig. 3a). The $[Ca^{2+}]_i$-increased region retracted and focal adhesions disappeared following the occurrence of $[Ca^{2+}]_i$ transient, as shown in the white arrowheads in Fig. 3a.

Analysis was performed on 113 cells. $[Ca^{2+}]_i$ transients were detected in 58 cells (51.3%). Most of these $[Ca^{2+}]_i$ transients displayed a Ca^{2+}-wave-like shape, initiated from the cell edges. Spatiotemporal properties were similar to those observed in spontaneous $[Ca^{2+}]_i$ transients. The frequency of $[Ca^{2+}]_i$ transients was 0.930 ± 0.182/cell/min (n = 17 independent experiments) during the $[Ca^{2+}]_i$ measurement period of 1–2 min. The peak value of F/F_0 was 2.51 ± 0.14 and the duration was 3.20 ± 0.17 s (n = 115 responses) in the 58 responding cells. This frequency was greater than four-fold higher than that of spontaneous $[Ca^{2+}]_i$ transients ($P < 0.01$). Moreover, the peak value of F/F_0 was also higher than that of spontaneous $[Ca^{2+}]_i$ transients ($P < 0.05$). Peak $[Ca^{2+}]_i$ levels in the majority of starting regions were greater than those levels evident at other regions. In the starting regions, rear retractions and inhibition of lamellipodium development were frequently observed following the occurrence of $[Ca^{2+}]_i$ transients (retraction, 52.1%; termination of extension, 15.5%). In contrast, extensions of the front edges were rarely observed (2.8%; Table 1). These results suggest that flow-induced $[Ca^{2+}]_i$ transients are closely associated with BAEC rear retraction under flow conditions.

To confirm the effects of fluctuations of cell thickness and localization of fluorescent probe on flow-induced $[Ca^{2+}]_i$ transients, changes in fluorescence on BAECs that loaded with Ca^{2+}-sensitive fura-red and Ca^{2+}-insensitive calcein were observed simultaneously (Fig. 4). Transient decreases in fura-red fluorescence were detected under flow conditions (Figs. 4a and 4b). Decreases in fura-red fluorescence indicate increases in $[Ca^{2+}]_i$. The spatiotemporal property was closely resemble that of $[Ca^{2+}]_i$ transient observed in fluo-4-loaded BAECs. However, changes in calcein fluorescence were not detected in the same cell. Differences of these changes in fluorescence clearly demonstrate that flow-induced $[Ca^{2+}]_i$ transients are not due to fluctuations of cell thickness and localization of fluorescent probes.

Effects of Gd^{3+} on $[Ca^{2+}]_i$ Transients and Retraction of Rear Edges under Flow Conditions

The effects of Gd^{3+} on $[Ca^{2+}]_i$ transients and rear retractions were examined (Fig. 5) in order to determine the mechanisms by which flow-induced $[Ca^{2+}]_i$ transients regulate rear retractions. In the presence of 30 μM Gd^{3+}, focal adhesions vanished on IRM images (33–60 min, Fig. 5a). Under this condition, relative retracted area was significantly reduced (0.24 ± 0.04%/min, n = 13 cells derived from 5 independent experiments; $P < 0.01$) as compared with control values (0.82 ± 0.09%/min, n = 17 cells derived from 4 independent experiments; Fig. 5b). Flow-induced $[Ca^{2+}]_i$ transients were also inhibited by Gd^{3+} (Fig. 5c). The percentage of responsive cells and the frequency of $[Ca^{2+}]_i$ transients were 8.3% and 0.154 ± 0.099/cell/min (n = 5 independent experiments), respectively. These values were lower than the comparable control values, 32.4% and 0.457 ± 0.051/cell/min (n = 4 independent experiments; $P < 0.05$), respectively. These results suggest that flow-induced rear retractions require $[Ca^{2+}]_i$ transients via mechanosensitive cation channels in BAECs.

Control values relating to the percentage of cells generating $[Ca^{2+}]_i$ transients and the frequency of $[Ca^{2+}]_i$ transients in the 31–32 min period were lower relative to those values representing the 0–1 min period (56.8% and 1.103 ± 0.131/cell/min; $P < 0.01$, respectively). Control values for relative retractions in the 33–60 min period were also smaller in comparison to those in the 3–27 min period (1.03 ± 0.11%/min; $P < 0.03$). Flow-induced $[Ca^{2+}]_i$ transients evoke retractions of their starting regions in which mechanical forces may be focused. Force-concentrated regions decreased with time upon the continuous application of flow. Consequently, the frequency and the response rate of $[Ca^{2+}]_i$ transients may be reduced.

Directional Rear Retractions Under Flow Conditions

The frequency of $[Ca^{2+}]_i$ transients was greater than fourfold higher than that of spontaneous $[Ca^{2+}]_i$ transients. Consequently, an increase in retracted areas under flow conditions, as compared with spontaneously retracted areas, should occur in the case where $[Ca^{2+}]_i$ transients are involved with rear retractions. However, no significant difference was observed in relative retraction under flow conditions in comparison to that of the spontaneous case (Figs. 2 and 5). The majority of spontaneous $[Ca^{2+}]_i$ transients were evident in regions displaying continuous retraction. In contrast, only 34% of flow-induced $[Ca^{2+}]_i$ transients occurred in regions exhibiting continuous retraction (data not shown). The $[Ca^{2+}]_i$ transient-induced retractile force may be antagonized by extensive force in cases where $[Ca^{2+}]_i$ transients occurred in regions which extended prior to the occurrence of $[Ca^{2+}]_i$ transients. Therefore, retracted areas may not always correlate with the frequency of $[Ca^{2+}]_i$ transients.

Distributions of retracted areas in the direction of flow were analyzed in order to ascertain the role of $[Ca^{2+}]_i$ transients on cell motility under flow conditions

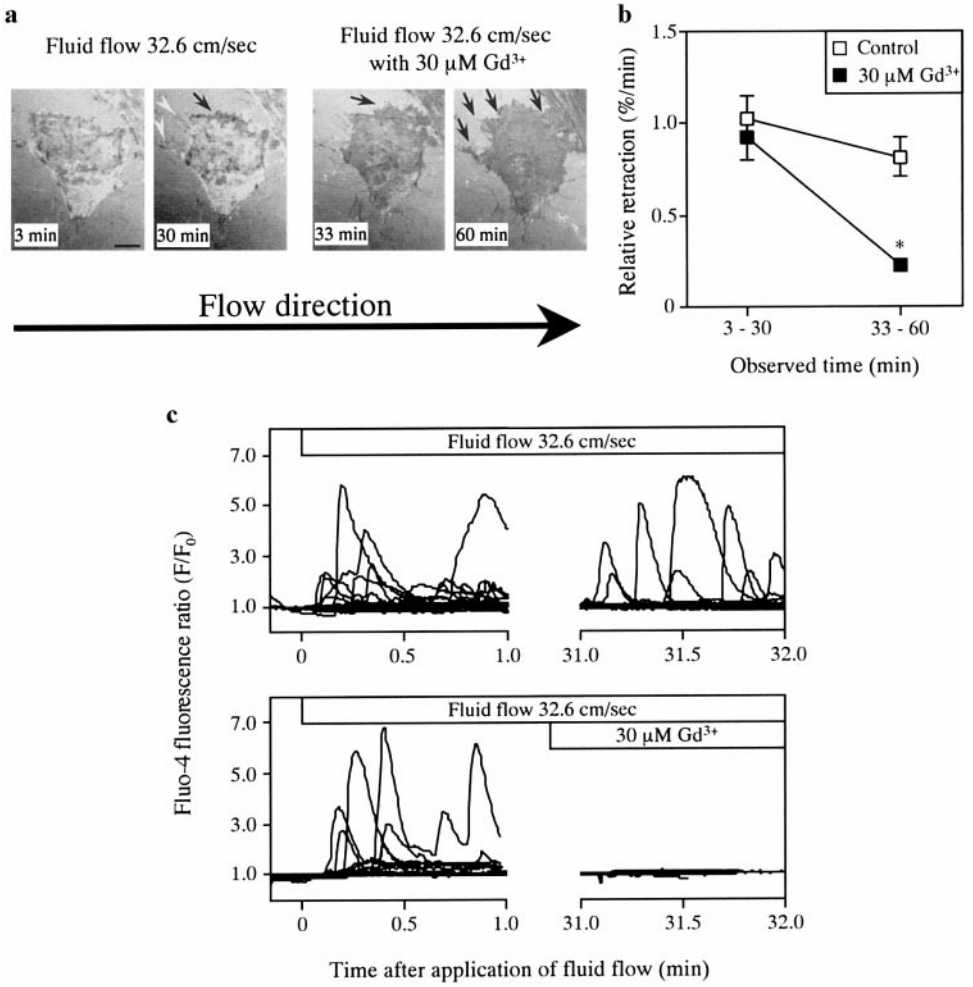

FIG. 5. Effects of Gd^{3+} on flow-induced $[Ca^{2+}]_i$ transients and rear edge retraction in BAECs. (a) IRM images illustrate typical changes in morphology in the presence of 32.6 cm/s fluid flow and 30 μM Gd^{3+}. Flow direction was left to right. Gd^{3+} was applied from 31 min. The white arrowheads indicate the disappearance of cell-substratum adhesion. The black arrows indicate extended lamellipodia. Scale bar represents 10 μm. (b) Effects of Gd^{3+} on rear edge retraction under flow conditions. Relative retraction was defined as the percentage of the retracted area for 27 min to the entire cell area at the initiation of each image. Values were determined from cells which responded during the $[Ca^{2+}]_i$ measurement period at 0–1 min and were normalized by time (min). Results were expressed as the mean ± SEM (control, n = 17 cells derived from 4 independent experiments; Gd^{3+}, n = 13 cells derived from 5 independent experiments). Statistical analysis was performed utilizing Student's t test; $^*P < 0.01$ compared with that of control. (c) Time course of F/F_0 changes of the entire cell in the presence of 32.6 cm/s fluid flow and 30 μM Gd^{3+} (upper, control; lower, Gd^{3+}). Each line represents data from different cells.

(Fig. 6). The ratio of the retracted area of the upstream region relative to the cell centroid to the entire retracted areas at 27 min was 0.66 ± 0.06 (n = 17 cells derived from 4 independent experiments; $P < 0.03$ compared with 0.5 at cell centroid). This value demonstrates the significant distribution of retracted areas in the upstream regions of cells under flow conditions. No directional retractions were observed in the presence of 30 μM Gd^{3+} (0.53 ± 0.06, n = 13 cells derived from 5 independent experiments; $P > 0.1$) or in the absence of fluid flow (0.53 ± 0.08, n = 16 cells derived from 12 independent experiments; $P > 0.1$). These results suggest that flow-induced $[Ca^{2+}]_i$ transients were required for retractions occurring in the upstream region, in particular. Furthermore, the findings indicate that biased retractions may be related to the directional migration of BAECs under flow conditions. These data appear to demonstrate the relationship between $[Ca^{2+}]_i$ transients and morphological responses of BAECs during the early phase of mechanotransduction.

It is well known that integrins, cell-substratum adhesion molecules, are clustered and localized in focal adhesions (16). EC adhesion to integrin $\alpha v\beta 3$ results in an elevation in $[Ca^{2+}]_i$. This rise in $[Ca^{2+}]_i$ stimulates EC migration on vitronectin, which is a specific substratum of integrin $\alpha v\beta 3$ (17). An increase in $[Ca^{2+}]_i$ was also apparent when integrins were subjected to stretch stimuli of a magnetic force (18). The rise in

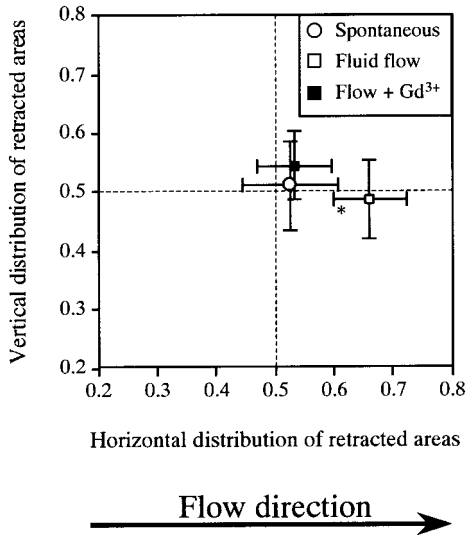

FIG. 6. Directional retraction of rear edges in BAECs under flow conditions. Fluid flow was applied from left to right for 27 min at 32.6 cm/s (fluid flow or flow + 30 μM Gd^{3+}). Distribution of retracted areas was defined as the ratio of the retracted areas, located in the left (upstream region in fluid flow or flow + Gd^{3+}; horizontal) or upper (vertical) regions toward the cell centroid, to the entire retracted area of the cell. Values of 0.5 represent the cell centroid. These values were obtained by analyzing the identical experiments shown in Fig. 2 (spontaneous) and Fig. 4 (fluid flow, flow + Gd^{3+}). Analyses were restricted to the responsive cells during the $[Ca^{2+}]_i$ measurement period of 1–2 min (spontaneous) or cells which responded during $[Ca^{2+}]_i$ measurement at 0–1 min (fluid flow and flow + Gd^{3+}). Results were expressed as the mean ± SEM (spontaneous, $n = 16$ cells derived from 11 independent experiments; fluid flow, $n = 17$ cells derived from 4 independent experiments; flow + Gd^{3+}, $n = 13$ cells derived from 5 independent experiments). Statistical analysis was performed using paired t test; $*P < 0.03$ compared with each 0.5 value representing the cell centroid.

$[Ca^{2+}]_i$ was blocked by the application of Gd^{3+}. This evidence suggests that integrins are involved in cell migration and mechanosensitive Ca^{2+} entry. Gd^{3+}-sensitive $[Ca^{2+}]_i$ transients, which were visualized in rear edges of BAECs, were associated with biased rear retractions. Moreover, starting regions of $[Ca^{2+}]_i$ transients corresponded to focal adhesion (Fig. 3). These observations support our results which indicate that flow-induced local $[Ca^{2+}]_i$ transients may also involve integrin, functioning as a mechanosenser, in order to evoke directional rear edge retraction.

It has been reported that migrating Chinese hamster ovary (CHO) cells require detachment of integrins at rear edges (19). Calpain, a calcium-dependent protease, is involved in the detachment of integrins (20). $[Ca^{2+}]_i$ transients were shown to regulate retraction of rear edges via the Ca^{2+}-sensitive phosphatase calcineurin in studies entailing the application of N-formyl-Met-Leu-Phe in chemotactic neutrophils (21). In this case, activated myosin II was localized at the rear edge of neutrophils and was associated with retraction (22). Myosin II is also involved in retraction in ECs (23). Consequently, our results strongly suggest that localized $[Ca^{2+}]_i$ transients, via a mechanosensitive cation channel, play an instrumental role in the detachment of integrin-mediated cell-substratum adhesion and/or actin-myosin based retraction.

ACKNOWLEDGMENT

We thank Dr. S. Shimizu of Showa University for kindly providing BAECs.

REFERENCES

1. Kohn, E. C., Alessandro, R., Spoonster, J., Wersto, R. P., and Liotta, L. A. (1995) Angiogenesis: Role of calcium-mediated signal transduction. *Proc. Natl. Acad. Sci. USA* **92,** 1307–1311.
2. Coomber, B. L., and Gotlieb, A. I. (1990) In vitro endothelial wound repair. Interaction of cell migration and proliferation. *Arteriosclerosis* **10,** 215–222.
3. Masuda, M., and Fujiwara, K. (1993) The biased lamellipodium development and microtubule organizing center position in vascular endothelial cells migrating under the influence of fluid flow. *J. Biol. Cell* **77,** 237–245.
4. Davies, P. F. (1995) Flow-mediated endothelial mechanotransduction. *Physiol. Rev.* **75,** 519–560.
5. Citi, S., and Kendrick-Jones, J. (1987) Regulation of non-muscle myosin structure and function. *Bioessays* **7,** 155–159.
6. Stolz, B., and Bereiter-Hahn, J. (1988) Increase of cytosolic calcium results in formation of F-actin aggregates in endothelial cells. *Cell Biol. Int. Rep.* **12,** 321–329.
7. Lawson, M. A., and Maxfield, F. R. (1995) Ca^{2+}- and calcineurin-dependent recycling of an integrin to the front of migrating neutrophils. *Nature* **377,** 75–79.
8. Schwartz, M. A. (1993) Spreading of human endothelial cells on fibronectin or vitronectin triggers elevation of intracellular free calcium. *J. Cell Biol.* **120,** 1003–1010.
9. Hendey, B., and Maxfield, F. R. (1993) Regulation of neutrophil motility and adhesion by intracellular calcium transients. *Blood Cells* **19,** 143–164.
10. Lee, J., Ishihara, A., Oxford, G., Johnson, B., and Jacobson, K. (1999) Regulation of cell movement is mediated by stretch-activated calcium channels. *Nature* **400,** 382–386.
11. Shimizu, S., Yamamoto, T., and Momose, K. (1993) Inhibition by methylene blue of the L-arginine metabolism to L-citrulline coupled with nitric oxide synthesis in cultured endothelial cells. *Res. Commun. Chem. Pathol. Pharmacol.* **82,** 35–48.
12. Davies, P. F., Robotewskyj, A., and Griem, M. L. (1993) Endothelial cell adhesion in real time. Measurements in vitro by tandem scanning confocal image analysis. *J. Clin. Invest.* **91,** 2640–2652.
13. Schwarz, G., Callewaert, G., Droogmans, G., and Nilius, B. (1992) Shear stress-induced calcium transients in endothelial cells from human umbilical cord veins. *J. Physiol.* **458,** 527–538.
14. Olesen, S.-P., Clapham, D. E., and Davies, P. F. (1988) Haemodynamic shear stress activates a K^+ current in vascular endothelial cells. *Nature* **331,** 168–170.
15. Hamill, O. P., and McBride, D. W., Jr. (1996) The pharmacology of mechanogated membrane ion channels. *Pharmacol. Rev.* **48,** 231–252.

16. Sjaastad, M. D., and Nelson, W. J. (1997) Integrin-mediated calcium signaling and regulation of cell adhesion by intracellular calcium. *BioEssays* **19,** 47–55.
17. Leavesley, D. I., Schwartz, M. A., Rosenfeld, M., and Cheresh, D. A. (1993) Integrin β1-and β3-mediated endothelial cell migration is triggered through distinct signaling mechanisms. *J. Cell Biol.* **121,** 163–170.
18. Glogauer, M., Ferrier, J., and McCulloch, C. A. G. (1995) Magnetic fields applied to collagen-coated ferric oxide beads induce stretch-activated Ca^{2+} flux in fibroblasts. *Am. J. Physiol.* **269,** C1093–C1104.
19. Palecek, S. P., Huttenlocher, A., Horwitz, A. F., and Lauffenburger, D. A. (1998) Physical and biochemical regulation of integrin release during rear detachment of migrating cells. *J. Cell Sci.* **111,** 929–940.
20. Huttenlocher, A., Palecek, S. P., Lu, Q., Zhang, W., Mellgren, R. L., Lauffenburger, D. A., Ginsberg, M. H., and Horwitz, A. F. (1997) Regulation of cell migration by the calcium-dependent protease calpain. *J. Biol. Chem.* **272,** 32719–32722.
21. Hendey, B., Klee, C. B., and Maxfield, F. R. (1992) Inhibition of neutrophil chemokinesis on vitronectin by inhibitors of calcineurin. *Science* **258,** 296–299.
22. Eddy, R. J., Pierini, L. M., Matsumura, F., and Maxfield, F. R. (2000) Ca^{2+}-dependent myosin II activation is required for uropod retraction during neutrophil migration. *J. Cell Sci.* **113,** 1287–1298.
23. Zeng, Q., Lagunoff, D., Masaracchia, R., Goeckeler, Z., Côté, G., and Wysolmerski, R. (2000) Endothelial cell retraction is induced by PAK2 monophosphorylation of myosin II. *J. Cell Sci.* **113,** 471–482.